Advanced Physical Research
Vol.7, No.3, 2025, pp.322-333
https://doi.org/10.62476/apr.73322

Jomard Publishing

INVESTIGATION OF THE CONDUCTIVE PROPERTIES OF $Ag_8Ge_{1-x}Mn_xTe_6$ SOLID SOLUTIONS

A.S. Gahramanova[1,2*], **R.N. Rahimov**[1], **D.G. Arasly**[1]
A.M. Karimova[1], **L.F. Valiyeva**[3]

[1]Institute of Physics, Ministry of Science and Education Republic of Azerbaijan, Baku, Azerbaijan
[2]Baku Business University, Baku, Azerbaijan
[3]Azerbaijan State Oil and Industry University, Baku, Azerbaijan

Abstract. Samples of $Ag_8Ge_{1-x}Mn_xTe_6$ solid solutions with varying manganese content ($x = 0, 0.05, 0.1, 0.2$) were synthesized by fusing and subsequently pressing the powdered precursors under a pressure of 0.6 GPa. X-ray diffraction analysis revealed that the introduction of manganese atoms led to a compression of the Ag_8GeTe_6 crystal lattice. All p-type samples exhibited high resistance below the transition region, with resistivity values measured in the temperature range of 180–220 K. The electrical conductivity of all compositions in the temperature range of 220–300 K increased via a hopping conduction mechanism, and for temperatures above 320 K, semiconductor-like behavior was observed. Impedance spectroscopy analysis showed that at 80 K, the solid solutions exhibited behavior characteristic of a homogeneous dielectric material. At elevated temperatures and under high-frequency external electric fields, the role of grain boundaries in electrical conductivity became significant. Additionally, the dielectric anomaly observed at low frequencies was attributed to the influence of grain boundary effect.

Keywords: Solid solutions, X-ray diffraction, DSC analysis, electrical conductivity, impedance spectra.
***Corresponding author:** A.S. Gahramanova, Institute of Physics, Ministry of Science and Education Republic of Azerbaijan, Baku, Azerbaijan, e-mail: *a.gahramanova@physics.science.az*
Received: 28 June 2025; Revised: 22 August 2025; Accepted: 28 August 2025; Published: 16 October 2025.

1 Introduction

Over the past few decades, the study of ionic crystals has become increasingly prevalent due to their extensive applications in electronics and energy technologies. Devices in these fields frequently rely on ion-conducting solid crystals. The investigation of ion transport processes in solid-state materials has significantly broadened the range of systems that exhibit ionic conductivity. As a result, ionic conductors are now widely employed in various devices used in electronics and power engineering (Hoang et al., 2025). These devices typically incorporate solid crystalline or polymer-based ionic conductors. The operation of such devices is fundamentally governed by electrochemical processes occurring both at the interface between the electrode and the ionic conductor and within the polycrystalline electrolyte itself. Among the most accessible and informative methods for investigating electrochemical and electrophysical phenomena in ion-conducting materials is impedance spectroscopy. This technique has become a valuable analytical tool across multiple disciplines, including electrochemistry, physics, and materials science. In recent years, scientifically validated approaches have been developed to obtain detailed insights not only into the intrinsic properties of the materials under investigation

but also into the mechanisms underlying the observed processes. Currently, impedance spectroscopy is primarily utilized to quantify ionic conductivity. For such measurements, a medium frequency range is typically sufficient. The ionically conductive ternary compound Ag_8GeTe_6, due to its complex crystal structure (Bendorius et al., 1975, Rysanek et al., 1976, Geller, 1979) and large unit cell, exhibits several unusual physical properties. These include low thermal conductivity, a narrow band gap (∼0.4 eV) (Fujikane et al., 2005), and superionic conductivity. Additionally, it demonstrates promising thermoelectric performance at temperatures of 500 K and above. Owing to these characteristics, Ag_8GeTe_6 is considered a prospective material for thermoelectric applications, functioning both as a converter of thermal energy into electrical energy and as an electrolytic material for energy storage in batteries. Consequently, in the last two decades, there has been growing interest in the study of such materials (Fujikane et al., 2005, Charoenphakdee et al., 2008, Zhu et al., 2010). It is well established that the properties of solid solutions and the temperatures of their phase transitions can be effectively tuned by varying their composition. Impurity atoms, which are part of the alloy, lead to violations of the potential field and periodicity of the crystal. A deformation region forms around defects and impurity atoms, which distorts the crystal lattice. Such distortions reduce the mean free path of phonons and charge carriers, thereby significantly altering the material's physical properties. In this study, new alloys were synthesized by adding highly soluble and diffusible manganese to the Ag_8GeTe_6 ternary compound. The incorporation of Mn atoms as magnetic impurities induces significant lattice distortions, which in turn affect the transport of phonons and charge carriers (Bekpulatov et al., 2025). Preliminary structural analyses indicate that the synthesized alloys retain the primary structure of AAg_8GeTe_6; however, the diffraction peaks for the composition containing 10% Mn exhibit a slight shift toward lower angles. This suggests that the incorporation of Mn leads to lattice compression in the host matrix (Gahramanova et al., 2018). Moreover, the addition of Mn results in the formation of a weakly antiferromagnetic material (Rahimov et al., 2021). In this article, we investigate the electrical conductivity under a constant electric field, as well as the impedance spectroscopy of the$Ag_8Ge_{1-x}Mn_xTe_6$ solid solution system.

2 Experimental

Solid solutions of $Ag_8Ge_{1-x}Mn_xTe_6$ ($x = 0, 0.05, 0.1, 0.2$) were synthesized in two stages. In the first stage, stoichiometric amounts of Ag, Ge, Te, and Mn were loaded into an ampoule, which was then evacuated to a pressure of 1.3 mPa and sealed. The ampoule was vibrated and gradually heated to 1250 K, held at this temperature for 4 hours, and then annealed at 900 K for 50 hours. In the second stage, the synthesized material was ground into powder using an agate mortar and passed through a 100-micron sieve. The sieved powder was placed into a parallelepiped-shaped steel mold and compressed under a pressure of 0.6 GPa. The resulting samples were annealed at approximately 800 K for 10 hours to achieve homogenization.

XRD analysis of the samples was conducted using a Bruker D2 Phaser diffractometer with CuK_α radiation over a $5 - -80^\circ$ 2θ range. Calorimetric studies were performed under an argon atmosphere in the 100–900 K temperature range using a NETZSCH DSC 204F1 Differential Scanning Calorimeter**.** Sapphire was used as a reference material, with a heating rate of 10 K/min and an argon gas flow rate of 20 mL/min.

Electrical conductivity and Hall coefficient measurements under constant electric and magnetic fields were carried out in the 80–700 K temperature range using the four-probe method. For frequency dependent specific conductivity measurements, disk-shaped samples with a diameter of 6 mm and a thickness of 1 mm were prepared. Silver paste was applied to the flat surfaces of the disks, and copper contacts were attached. The frequency dependence of specific conductivity and capacitance was measured using a Precision LCR Model 1920 (IET Labs). The applied voltage during the measurements was 200 mV. Based on the measured capacitance

and conductivity data, the real and imaginary parts of the dielectric constant were calculated.

Experimental results were analyzed using an equivalent circuit model with a parallel RC contour. Frequency-dependent impedance measurements were also conducted at room temperature and at 80 K (liquid nitrogen temperature).

3 Results and discussion

The diffraction patterns of the $Ag_8Ge_{1-x}Mn_xTe_6$ solid solutions ($x = 0, 0.1, 0.2$) are presented in Figure 1. Investigations indicate that the synthesized solid solutions exhibit a crystal structure identical to that of the Ag_8GeTe_6 ternary compound. However, for compositions containing 10% and 20% manganese, the diffraction peaks exhibit slight shifts toward lower angles, suggesting that the incorporation of manganese atoms induces a minor lattice expansion (Tran et al., 2025). As shown in Figure 1, in the sample with x = 0.20, all major diffraction peaks correspond to the Ag_8GeTe_6 ternary compound, while the relatively intense reflections at 28.8° and 31.5°, along with other weaker reflections, are presumed to correspond to the $MnTe_2$ phase (Szwacki et al., 2004, Ibaeva et., 2024).

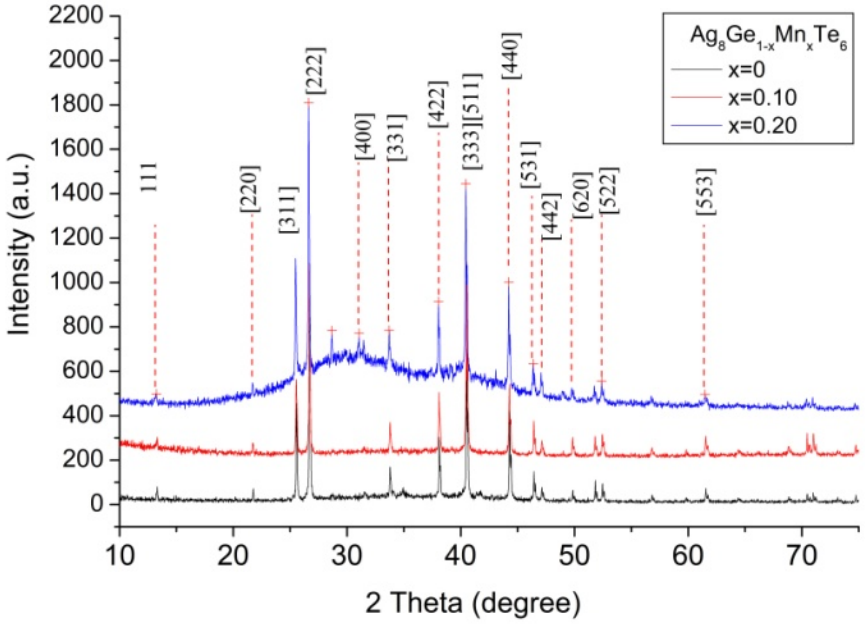

Figure 1: XRD patterns of the $Ag_8Ge_{1-x}Mn_xTe_6$ solid solutions.

It should be noted that the information in the literature regarding the low-temperature structure of Ag_8GeTe_6 is ambiguous. The compound is reported to belong to a space group, with a lattice constant is a = 11.58 ± 0.02A (Bendorius et al., 1979, Ibragimov., et al, 2024). According to Geller's research (Geller, 1979), the Ag_8GeTe_6 compound belongs to the F43m space group with $Z = 4$ and a lattice constant of a = 11.58 ± 0.02Å. In studies (Gaudin et al., 2000), it is shown that compounds belonging to the argyrodite family exhibit numerous structural transitions at temperatures below room temperature. According to the studies by Kawaji and Atack, four transitions are observed in the Ag_8GeTe_6 compound: first-order (structural) transitions at 223K and 245K, and second-order transitions at 156K and 170K (Kawaji & Atake, 1994). Some authors, however, consider all transitions to be first-order, while others suggest that these transitions are related to the ordering of Ag^+ ions (Evain et al., 1998, Gaudin et al., 2000).

To identify the structural changes induced by manganese in the $Ag_8Ge_{1-x}Mn_xTe_6$ alloys, Differential Scanning Calorimetry (DSC) was employed to study variations in heat flow within

the samples. The DSC curve of the $Ag_8Ge_{1-x}Mn_xTe_6$ ($x = 0, 0.05, 0.1, 0.2$) solid solutions presented in Figure 2. As seen in the Ag_8GeTe_6 compound endothermic peaks are observed at 225 K, 243 K, and 638 K. Similarly, in the $Ag_8Ge_{1-x}Mn_xTe_6$ solid solutions, the same two endothermic peaks below room temperature are present. However, additional endothermic peaks are observed above room temperature, approximately at 340 K and 626 K.

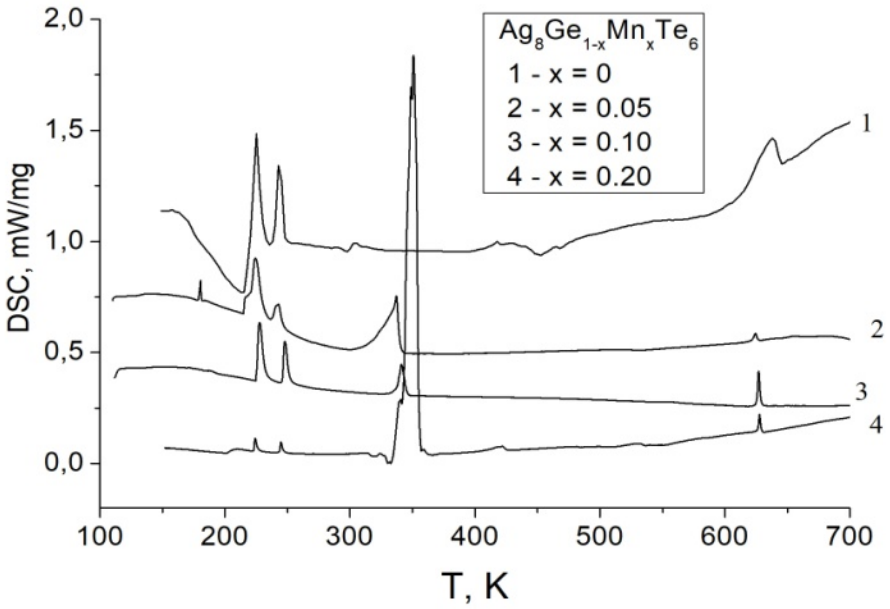

Figure 2: Results of DSC analysis for $Ag_8Ge_{1-x}Mn_xTe_6$ solid solutions.

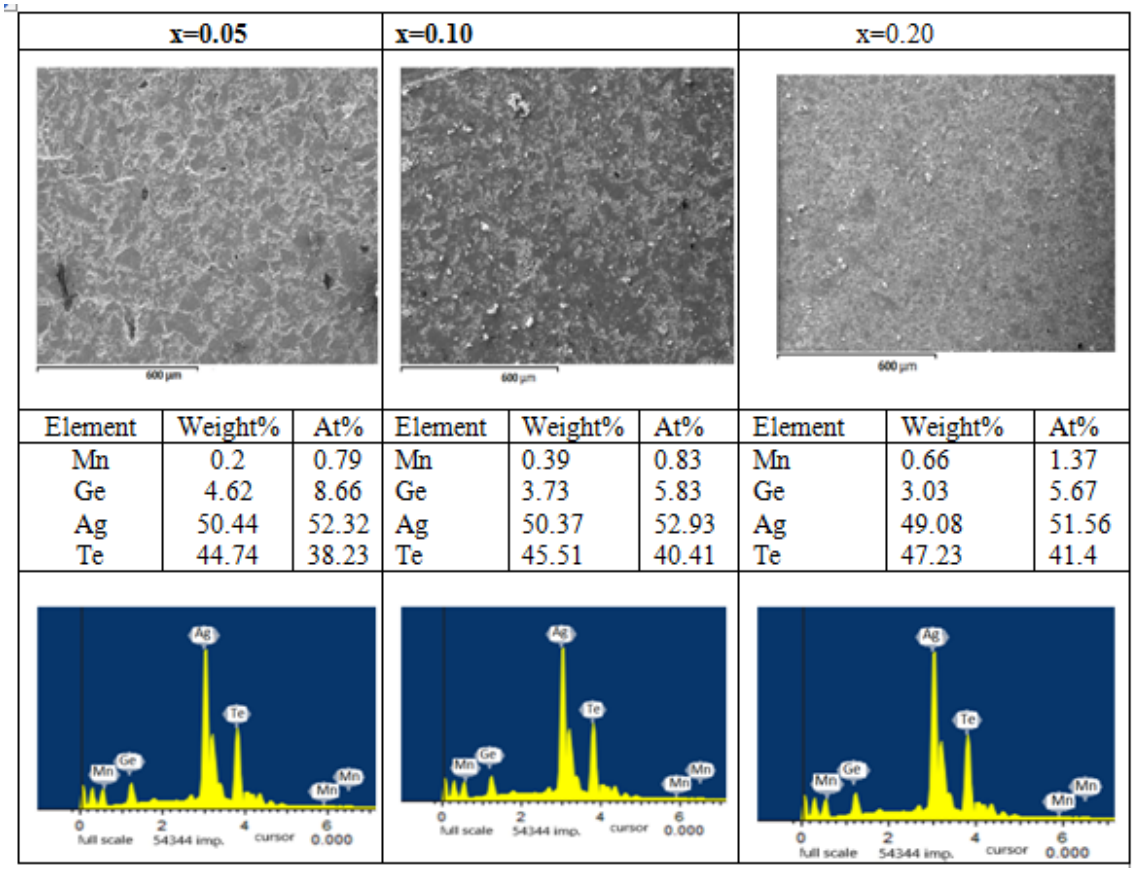

Figure 3: Elemental analyses for $Ag_8Ge_{1-x}Mn_xTe_6$ alloys ($x = 0.05, 0.1 and 0.2$).

As shown in Figure 3, elemental analysis performed using a "JEOL 6610LV SEM" confirms that the composition corresponds to that of the solid solution. Electrical conductivity measurements of $Ag_8Ge_{1-x}Mn_xTe_6$ alloys ($x = 0, 0.05, 0.1, and 0.2$) were carried out under a static electric field in the temperature range of 100–650 K. The results are presented in Figure 4(a) and 4(b) with the inset showing the dependence of $ln(T^{-1/4})$.

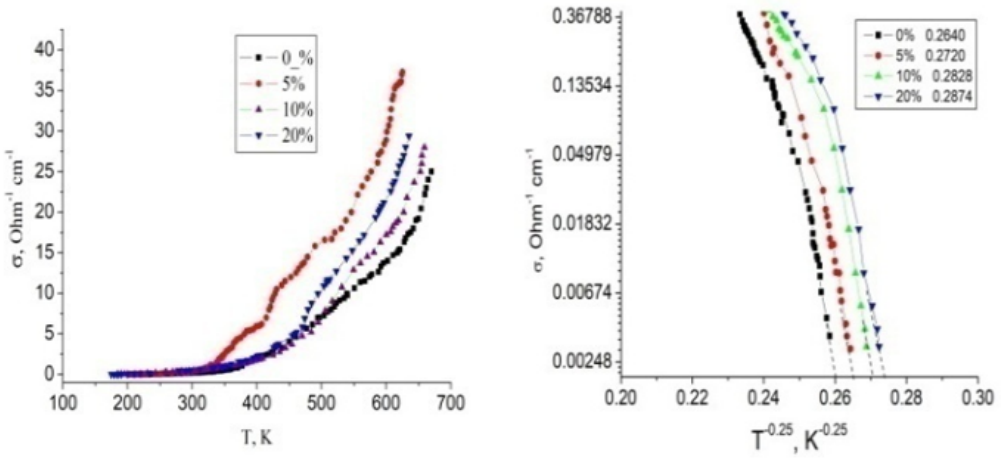

Figure 4: a - Temperature (T,K) dependence conductivity of $Ag_8Ge_{1-x}Mn_xTe_6$ solid solutions; Temperature ($T^{0.25}$,$K^{0.25}$) dependence conductivity of $Ag_8Ge_{1-x}Mn_xTe_6$ solid solutions.

All samples exhibit high resistivity at temperatures below 180 K. In the temperature range of 200–650 K, the electrical conductivity of all samples demonstrates activated behavior, increasing by nearly two to three orders of magnitude. It is noteworthy that in the temperature range of 180–300 K, the conductivity exhibits a hopping mechanism. According to Mott's theory (Mott, 1969), electrical conduction in this regime occurs via a hopping between localized states situated within a narrow energy band near the Fermi level. Transport through these localized states results from charge carriers hopping from one localized site to another.

Hopping conduction typically occurs in compensated semiconductors at low temperatures, involving transitions between nearest neighboring sites. In cases of weak donor compensation within the impurity band, the density of states as a function of energy exhibits a maximum corresponding to the ionization energy of the most isolated donor. When the initial and final hopping sites are spatially close, their energies approximate this maximum density of states. For a hopping event to occur, the target site must be unoccupied. The hopping conductivity strongly depends on impurity concentration and typically follows an exponential relationship, which serves as key experimental evidence supporting this conduction mechanism.

Accordingly, we analyzed the temperature dependence of the electrical conductivity, σ(T), in the 220–300 K range using Mott's variable-range hopping (VRH) relation (Mott 1969; Fateev, 2010):

$$\sigma(T) = \sigma_0 \exp\left[-\left(\frac{T_0}{T}\right)^{1/4}\right] \tag{1}$$

where $T_0 = \beta/g(\mu)r^3k_B$, $g(\mu)$ is the density of localized states at the Fermi level, r is the radius of localized states near the Fermi level, k_B is Boltzmann's constant, and β depends on the dimensionality of the system ($\beta = 21$ in three dimensions (Ragimov et al., 2020)). The data yield linear Mott plots in the specified temperature range, indicating that charge transport in this regime occurs via hopping between localized states near the Fermi level. Structural disorder, interstitial impurities, vacancies, and dislocations disrupt the periodicity of the crystal lattice, creating localized states with in the band gap of an ideal crystal. As shown in Figure 4, the

Mott relation (1) is valid in the 220–300 K temperature range for Ag_8GeTe_6. The value of T_0 is determined by the inclination of the line in the coordinates $ln(T^{-1/4})$:

$$T_0^{1/4} = \frac{\ln \sigma_1 - \ln \sigma_2}{T_1^{1/4} - T_2^{1/4}} \tag{2}$$

Using the experimental data, we calculated the density of localized states $g(\mu)g(\mu)g(\mu)$ for the $Ag_8Ge_{1-x}Mn_xTe_6$ solid solutions as follows: $Ag_8Ge_{1-x}Mn_xTe_6$: $g(\mu) = 1,378 \times 10^{18}\, eV^{-1}cm^{-3}$ (for $x = 0$); $g(\mu) = 1.684 \times 10^{19}\, eV^{-1}cm^{-3}$ (for $x = 0.05$); $g(\mu) = 6,381 \times 10^{18} eV^{-1}cm^{-3}$ (for $x = 0.1$) and $g(\mu) = 4,06 \times 10^{19} eV^{-1}cm^{-3}$ (for $x = 0.2$). These results support the assumption that, in this temperature range, charge transport in these materials occurs through hopping between localized states in a narrow energy band near the Fermi level (Ibayeva et al., 2025).

Given the granular nature of the studied samples, grain boundaries play a significant role in charge transport via the hopping mechanism. Grain size calculations based on the Debye–Scherrer model indicate that the average grain size in these solid solutions is approximately $1.5\mu m$. Charge accumulation at intergranular boundaries can significantly influence conductivity and alter the dielectric properties of the material. The effect of grain boundaries on conductivity can be further investigated using alternating current (AC) measurements. Impedance spectroscopy provides valuable insights into charge transport mechanisms by accounting for the microstructure of the sample, transport properties in layered structures (Sardarly et al., 2014), phase transitions in ionic crystals (Alekperov et al., 2015), the impact of impurities on electrophysical properties in doped materials (Ivanov et al., 2000), and the role of crystallites and their interfaces in electrical conductivity (Yakimchuk et al., 2005).

The frequency-dependent dielectric permittivity of $Ag_8Ge_{1-x}Mn_xTe_6$ solid solutions ($x = 0, 0.05, 0.1$, and 0.2), calculated from experimental conductivity and capacitance data, is presented in Figure 5(a) and 5(b) for temperatures of 80 K and 300 K, respectively. At 80 K, the sample with 5% manganese exhibits a maximum dielectric permittivity (ε) of 40 at 20 Hz, decreases to 30 at a frequency of 2×10^5 Hz. At 300 K, these values increase anomalously. The sharp rise in permittivity with increasing temperature is attributed to the enhanced concentration of ionic charge carriers at elevated temperatures.

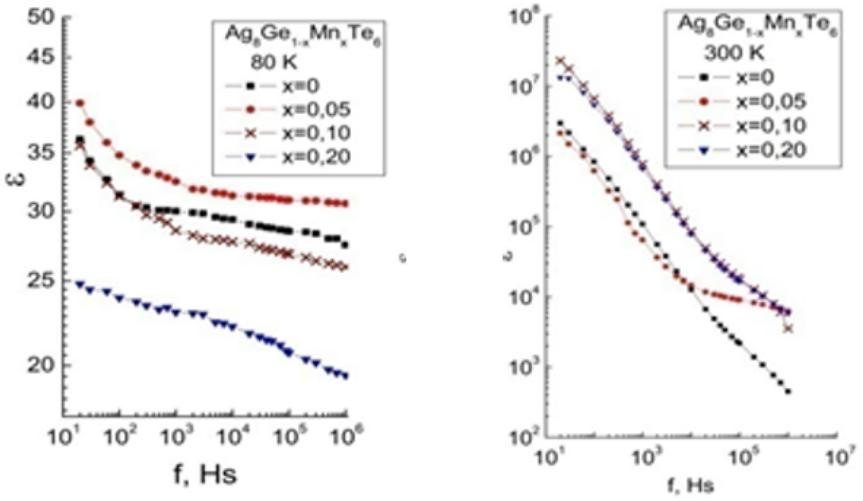

Figure 5: a - The dependencies of the dielectric permittivity of $Ag_8Ge_{1-x}Mn_xTe_6$ solid solutions at 80 K; b-The dependences of the dielectric permittivity of $Ag_8Ge_{1-x}Mn_xTe_6$ solid solutions at 300 K.

For the solid solution $Ag_8Ge_{1-x}Mn_xTe_6$ ($x = 0 to 0.2$), the frequency dependence of the real part Z′ and the imaginary part Z′ of the impedance is presented in Figure 6. At 80 K, the $Z\prime(f)$

component exhibits a more pronounced decrease (from 10^9 Ohm to 10^2 Ohm) compared to the $Z\prime(f)$ component, which decreases from 10^9 Ohm to 10^4 Ohm. At 300 K, the Z$\prime$(f) dependence changes very slightly up to a frequency of 10^5 Hz, after which it begins to decrease. For the composition with $x = 0.05$, this decrease is more significant. Conversely, the $Z\prime\prime(f)$ component increases with frequency at 300 K. At this temperature, $Z\prime\prime(f)$ exceeds $Z\prime(f)$, and their ratio varies from approximately hundred to one with increasing frequency.

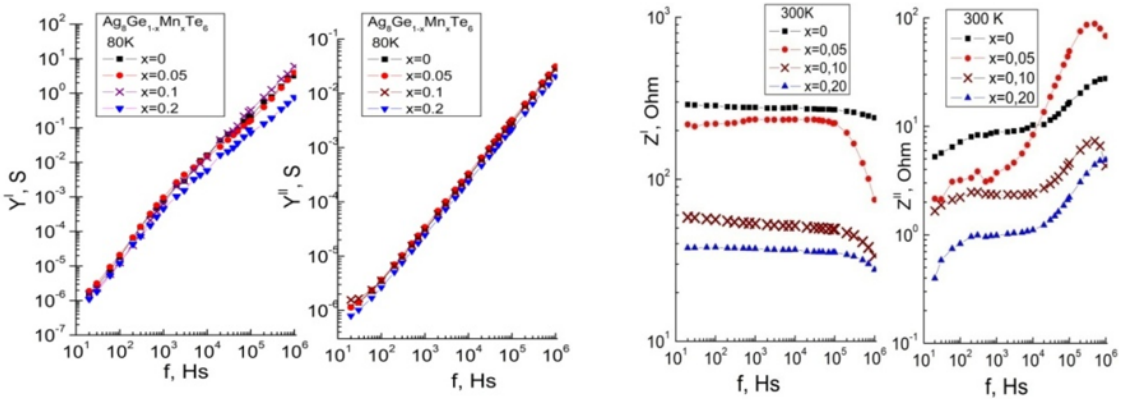

Figure 6: a-Frequency dependencies of the real Z' and imaginary parts Z'' of the impedance at 80K$Ag_8Ge_{1-x}Mn_xTe_6$ solid solutions; b- Frequency dependencies of the real Z' and imaginary parts Z'' of the impedance at 300 K for $Ag_8Ge_{1-x}Mn_xTe_6$ solid solutions.

To gain insight into the polarization mechanism in the investigated solid solutions, impedance spectroscopy (i.e., analysis of the dependence of $Z\prime\prime$ on $Z\prime$) was performed. Figure 7 presents the Nyquist plots (hodographs) at temperatures of 80 K and 300 K. At 80 K, the Nyquist plots pass through the origin and form semicircular arcs. The arc radii differ depending on the composition: the smallest radius is observed for x = 0.1, while the largest is for x = 0.2. Such behavior suggests that the material is homogeneous at this temperature. At 300 K temperature two arcs of circles are observed in the hodograph, the sites of which are shifted from the Z^I axis and with an increasing composition approaching the origin of coordinates. It is important to note that no form of lattice polarization is expected in this frequency range. Typically, the high-frequency arc corresponds to charge transport within the grain volume, and the arc corresponding to lower frequencies reflects the contribution of the intercrystalline boundary (Ivanov-Shits et al., 2000). An equivalent circuit of such a spectrum is a parallel RC circuit.

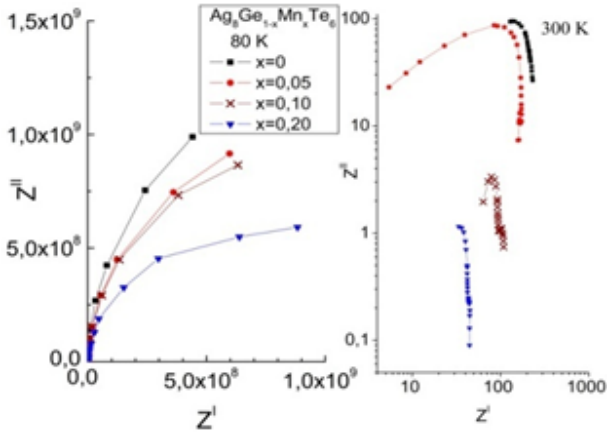

Figure 7: a,b-The hodograph at 80 K and 300 K for $Ag_8Ge_{1-x}Mn_xTe_6$ solid solutions.

The dielectric anomaly observed at low frequencies is also associated with effects occurring

at intergranular boundaries (Irvine et al., 1990). Charges accumulate at the grain boundaries, altering the dielectric constant of the material. According to the authors (Zukovskiy et al., 1997), at low temperatures, the majority of defects reside in a neutral charge state. As the temperature increases, charge exchange between defects can occur via hopping Mechanisms. As the temperature increases, charge exchange occurs between defects through hopping processes. A defect becomes temporarily charged and subsequently returns to its neutral state. This dynamic, where in the charge state of defects changes via hopping, creates deep levels within the forbidden energy gap and leads to an increase in dielectric permittivity under an external electric field.

In heterogeneous systems with dielectric constant exceeding 1000 at low frequencies, the role of grain boundaries in polarization can be analyzed using the concept of the "electrical module" (Kudryashov et al., 2014). To correlate the features observed in impedance spectra with capacitance behavior, complex conductivity or the electric modulus has been calculated using the standard formulas (3) and (4).

$$Y = \frac{1}{Z^I(f) + iZ^{II}(f)} = \frac{Z^{II}}{Z^2} - i\frac{Z^{II}}{Z^2} = Y^I(f) - iY^{II}(f) \tag{3}$$

$$Y^{II} = \sim\omega C_{ef} \tag{4}$$

The results derived from these expressions are presented in Figure 8.

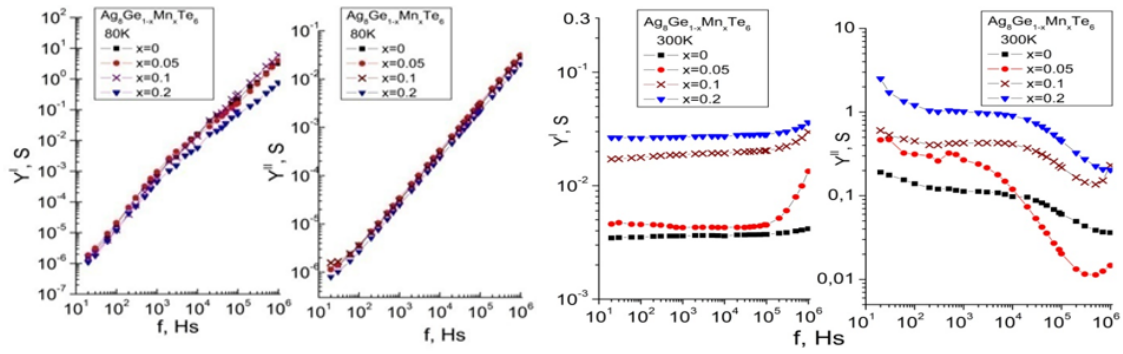

Figure 8: a- The real Y^I and imaginary parts Y^{II} of the complex conductivity at 80 K for $Ag_8Ge_{1-x}Mn_xTe_6$ solid solutions; b-The real Y^I and imaginary parts Y^{II} of the complex conductivity at 300 K for $Ag_8Ge_{1-x}Mn_xTe_6$ solid solutions.

At a temperature of 80 K, the real and imagunary parts of the complex conductivity follows a frequency dependence of $Y^I \sim f^{0.96}$. This indicates that the effective capacitance parameter C_{ef} shows very weak frequency dependence, according to Equation (4). For the solid solutions $Ag_8Ge_{1-x}Mn_xTe_6$ ($x = 0, 0.05, 0.10$), the reduced capacitance C_{ef}/C_0 (where $C_0 = \epsilon_0 S/d$ - is the geometric capacitance of the sample, ϵ_0- is the absolute dielectric constant, S is the contact area, d is the distance between contact) has values ranges from 27 to 38 at 80 K and low frequencies, as seen in Figure 9. At frequencies above 500 Hz, the effective capacitance remains stable for all compositions. This behavior indicates that, at 80 K, the solid solutions act as homogeneous dielectric materials. Indeed, in a homogeneous system, the parameter C_{ef} would correspond to the capacitance C of flat capacitor with dielectric constant ε. At 300 K and low frequencies, the value of C_{ef}/C_0 ratio reaches approximately 10^7 , then decreases by three or four orders of magnitude as frequency increases, whereas for a solution with composition x=0.05, this ratio becomes constant for $f > 20$ kHz. Therefore, the parameter C_{ef}/C_0 cannot be considered a reliable measure of the dielectric constant of the material. The parameter calculated using expression (4) is significantly large within the examined temperature range, and due to its strong frequency dependence, it cannot be interpolated as the material's dielectric constant. In practical

terms, while the parameter Y^I remains nearly unchanged, the measured capacitance decreases with increasing frequency and approaches a limiting value. The extremely high capacitance values observed at low frequencies cannot be attributed solely to lattice polarization. The frequency corresponding to the observed effect is much higher than the frequencies at which the measurements were conducted.

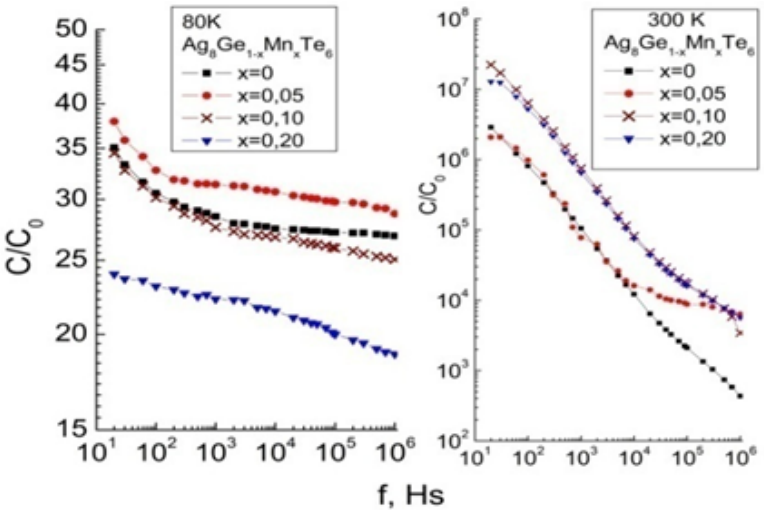

Figure 9: Frequency dependencies of the specific capacitance (C_{ef}/C_0) at 80 K and 300 K for $Ag_8Ge_{1-x}Mn_xTe_6$ samples.

It is important to note that a decrease in capacitance with decreasing frequency is frequently observed. In many cases, capacitance decreases with increasing frequency. Under such conditions, the effective capacitance at low frequencies becomes anomalously high, and the recalculated value of capacitance (C_{ef}/C_0) exceeds $10^3 - 10^4$. At frequencies below 10^{12} Hz, such behavior cannot be attributed to conventional polarization mechanisms namely ionic, electronic, or orientational polarization since these are associated with rapid electronic processes.The authors of (Lunkenheimer et al., 2002) have shown that even in systems where dipole moments do not form due to the characteristics of the crystal lattice, anomalously high capacitance can be observed as a result of structural inhomogeneity. Accordingly, the C_{ef}/C_0 parameter, calculated using Equation (3), becomes significantly large and exhibits a strong frequency dependence within the given temperature range. In contrast to the practically unchanged parameter Y^I, described capacitance decreases with an increasing frequency and approaches the value. Under an alternating electric field, charge redistribution occurs gradually within the electronic subsystems between crystallites, giving rise to additional capacitance at low frequencies. As the frequency increases, this contribution diminishes, and the high-frequency capacitance converges to the intrinsic dielectric constant of the material.This phenomenon is commonly referred to as the Maxwell–Wagner effect in the literature. In polycrystalline materials, such effects can arise due to polarization processes occurring in the intercrystalline regions (Adams et al., 2006). As the frequency of the external field increases, the slowest repolarization processes associated with structurally inhomogeneous regions become "frozen." Consequently, the contribution of these relaxation processes particularly those involving charge carriers near structural inhomogeneities to the overall capacitance decreases with increasing frequency.

4 Conclusion

X-ray diffraction (XRD) and differential scanning calorimetry (DSC) analyses were employed to confirm the structural identity of $Ag_8Ge_{1-x}Mn_xTe_6$ solid solutions ($x = 0, 0.05, 0.1, 0.2$) in comparison with the Ag_8GeTe_6 ternary compound. The incorporation of manganese atoms

into the Ag_8GeTe_6 framework led to lattice compression and the formation of a deformation field, resulting in a changes in lattice periodicity. Due to the anharmonicity of the lattice vibrations, the alloy exhibits low thermal conductivity. Impedance spectroscopy revealed that at liquid nitrogen temperatures, the complex conductivity increased with the frequency of the external electric field following the relation $Y_I \sim f^{0.96}$. At 80 K, the reduced capacitance remained nearly constant at frequencies above 100 Hz, suggesting that the solid solution behaves as a homogeneous dielectric material at low temperatures. At room temperature, the reduced capacitance exhibited anomalously high values at low frequencies, which decreased by three to four orders of magnitude as the frequency increased. Complex conductivity at room temperature remained constant up to a frequency of 10^5 Hz. These observations highlight the significant role of intergrain boundaries in the electrical conductivity and dielectric response of the material.

References

Adams, T.B., Sinclair, D.C. & West, A.R. (2006). Characterization of grain boundary impedances in fineand coarse-grained $CaCu_3Ti_4O_{12}$ ceramics. *Physical Review B*(73), 094124. https://doi.org/10.1103/PhysRevB.73.094124

Alekperov, O., Samedov, O., Paucar, R., Abdulzade, N., Nakhmedov, E., Nadjafov, A., Wakita, K., & Mamedov, N.(2015). Impedance spectroscopy study of phase transitions toionic and superionic conductivity states in Ag2S andAg2Se. *Physica Status Solidi(a), 252*(A206), 610-614. https://doi.org/10.1002/pssc.201400366

Bendorius, R., Irzikevicius, A., Kindurys, A. & Tsvetkova, E.V. (1975). The absorption spectra of $Ag_8M_4Se_6$ and Ag_8GeX_6 VI compounds. *Physica Status Solidi(a), m28*(2), K125-K127. https://doi.org/10.1002/pssa.2210280245

Bekpulatov, I.R., Imanova, G.T., Nabiev, D.Kh., Igamov, B.D., Kamardin, A.I., Jabbarov, S.H., & Aliyev, Y.I., (2025). Study of the electrophysical properties of higher managanase silicide (Mn_4Si_7) thin films and their temperature dependence. *Ceramics International, 51*(14), 19145-19155. https://doi.org/10.1016/j.ceramint.2025.02.093

Charoenphakdee, A., Kurosaki, K., Muta, H., Uno, M. & Yamanaka, S. (2008). Reinvestigation of the thermoelectric properties of Ag_8GeTe_6. *Physica Status Solidi RRL 2*(2), 65–67. https://onlinelibrary.wiley.com/doi/pdf/10.1002/pssr.200701302

Evain, M., Gaudin, E., Boucher, F., Petricek, V. & Taulellec, F. (1998). Structures and phase transitions of the A_7PSe_6 (A = Ag, Cu) argyrodite-type ionic conductors. I. Ag_7PSe_6. Structural Science, *Crystal Engineering and Materials*, B54, 376-383. https://doi.org/10.1107/s0108768197019654

Fateev, M.P. (2010). Theory of hopping transfer in disordered systems. *Physics of the Solid State*, 52, 1123-1130. https://link.springer.com/article/10.1134/S106378341006003X

Fujikane, M., Kurosaki, K., Muta, H. & Yamanaka, S. (2005). Thermoelectric properties of Ag_8GeTe_6. *Journal of Alloys and Compounds, 396*(1–2), 280–282. https://doi.org/10.1016/j.jallcom.2004.12.038

Gahramanova, A., Qasymov, V., Khalilova, A., & Rahimov, R. (2018). Thermodynamic Properties of $Ag_8Ge_{1-x}Mn_xTe_6$ Alloys. *7th Rostocker International Conference: Thermophysical Properties for Technical Thermodynamics*, Rostock, Germany, 73-74.

Gaudin, E., Boucher, F., Petricek, V., Taulellec, F. & Evain, M. (2000). Structures and phase transitions of the A_7PSe_6 (A = Ag, Cu) argyrodite-type ionic conductors. II. β- and γ-

Cu_7PSe_6. *Structural Science, Crystal Engineering and Materials*, B56, 402-408. https://journals.iucr.org/b/issues/2000/03/00/lc0017/lc0017.pdf

Gaudin, E., Boucher, F., Petricek, V., Taulellec, F. & Evain, M. (2000). Structures and phase transitions of the A_7PSe_6 (A = Ag, Cu) argyrodite-type ionic conductors. III. α- Cu_7PSe_6. Structural Science, Crystal Engineering and Materials, B56, 972-979. https://doi.org/10.1107/S0108768100010260

Geller, S. (1979). The crystal structure of γ Ag_8GeTe_6, a potential mixed electronic-ionic conductor. Zeitschriftfür für-Kristallographie Crystalline Materials, 149(1-2), 31-47. https://doi.org/10.1524/zkri.1979.149.1-2.31

Hoang, T.P., Truong-Son, L.V., Phan, L., Nghiem, N.T., Truong-Tho, N., Tiep, N.H., ... , Khan, D.T. (2025). Structural, Magnetic and Ferroelectric Phase Transsitions and Energy Storage Efficiency in Ba_{1-x} La_xTi_{1-x} Fe_xO_3 Ceramics. *Journal of Electronic Materials*, 54, 929-943. https://doi.org/10.1007/s11664-024-11593-w

Irvine, J.T.S., Sinclair, D.C., & West, A.R. (1990). Electroceramics: Characterization by Impedance Spectroscopy. *Advanced Materials, 2*(3), 132–138.

Ivanov-Shits, A.K., Murin, I.V. (2000). *Ionica tverdogo tela*. Saint-Petersburg, 617p.(in Russian)

Ibaeva, R.Z., Ibragimov, G.B., Alekperov, A.S, & Huseynov, R.E. (2024). Obtained and Studied Structural Aspects of the Ge0.9Er0.1S Compound with Ge → Er Substitutions. *East European Journal of Physics*, 4, 360-363. https://doi.org/10.26565/2312-4334-2024-4-41

Ibaeva, R.Z, Ibragimov, G.B., & Ibragimov, B.G. (2025). Optical absorption in quantum dot superlattices with parabolic potential. *Radioelectronics. Nanosystems. Information Technologies, 17*(3), 301-304. https://doi.org/10.17725/j.rensit.ru.2025.17.301

Ibragimov, G.B., Ibaeva, R.Z., Alekperov, A.S, & Ibragimov, B.G. (2024). Light absorption by fre charge carriers in the presence of phonons in an anisotropic quantum wire, *Advanced Physical Research 6*(1), 56-62. https://doi.org/10.62476/apr61.62

Jana, P.K., Sarkar, S., & Chaudhuri, B.K. (2007). Maxwell-Wagner polarization mechanism in potassium and titanium doped nickel oxide showing giant dielectric permittivity. *Journal of Physics:Applied Physics* 40, 556-560. https://doi.org/10.1088/0022-3727/40/2/033

Kudryashov, M.A., Mashin, A.I., Logunov, A.A., Chidichimo, G. & Filpo, G.De. (2014). Dielectric Properties of Ag/PAN Nanocomposites. *Technical Physics, 59*(7), 1012–1016. https://doi.org/10.1134/S1063784214070147

Kawaji, H., Atake, T. (1994). Heat capacity measurement and thermodynamic study of Ag_8GeT_{e6}. Solid State Ionics, 70(1), 518-521. https://doi.org/10.1016/0167-2738(94)90364-6

Lunkenheimer, P.,Bobnar, V., Pronin, A.V., Ritus, A.I., Volkov, A.A., & Loidl, A. (2002) Origin of apparent colossal dielectric constants. *Phys. Rev., B66*(5), 052105, 422. https://doi.org/10.1103/PhysRevB.66.052105

Mott, N.F. (1969). Conduction in non-crystalline materials. *The Philosophical Magazine: A Journal of Theoretical Experimental and Applied Physics, 19*(160), 835-852. ttps://doi.org/10.1080/14786436908216338

Ragimov, S.S., Saddinova, A.A., Alieva, A.I., & Selim-zade R.I.(2020) Hopping Conduction in $AgSbSe_2$ and $(AgSbSe_2)_{0.9}(PbTe)_{0.1.}$. Inorganic Materials 56, 779-784. https://link.springer.com/journal/10789

Rysanek, N., Laruelle, P. & A. Katty. (1976). Structure cristalline de Ag_8GeTe_6 (γ). *Acta Crystallografica*, B32, 692-696. https://journals.iucr.org/b/issues/1976/03/00/a13192/a13192.pdf

Rahimov, R., Yanushkevich, K., Khalilova, A., Gahramanova, A., Mammadov, I., Arasly, D., ... & Rimskiy, G. (2021). Specific magnetization and magnetic susceptibility $Ag_8Ge_{0.8}Mn_{0,2}Te_6$. 10th Rostocker International Conference: Thermophysical Properties for Technical Thermodynamics, 09-10 September, Rostock, Germany, 143. https://www.ltt.uni-rostock.de/storages/uni-rostock/Alle_MSF/LTT/Thermam/Abstract_Book_THERMAM_2021.pdf

Sardarly, R. M., Samedov, O. A., Alieva, N. A., Abdullayev,A. P. , Huseynov, E. K., Hasanov, I. S. & Salmanov, F. T. (2014). On the polarization caused by bulk charges and the ionic conductivity in $TlInSe_2$ crystals Semiconductors, 48(4), 427–431. https://doi.org/10.1134/s1063782614040253

Szwacki, G.N., Przeździecka, E., Dynowska, E., Bogusławski, P., & Kossut, J. (2004). Structural Properties of MnTe, ZnTe, and ZnMnTe. *Acta Physica Polonica A, 106*(2), 233-238.

Tran, T.A., Nguyen, T.H., Tien, D.P.T., Nguyen, L.V.T., Hoang, T.P., Nguyen, T.T., ... & Nguyen, V.T. (2025). Sol-gel synthesis, characterization and catalytic activity of manganese-doped calcium cobalt oxide. Next Materials, 8, 100843. https://doi.org/10.1016/j.nxmate.2025.100843

Yakimchuk, A.V., Zaikina, J.V., Reshetova, L.N., Ryabova, L.I., Khokhlov, D.R. & Shevelkov, A.V. (2007). Impedance of $Sn_{24}P_{19.3}Br_xI_{8-x}$ semiconducting clathrates. *Low Temperature Physics, 33*(2–3), 276-279. https://doi.org/10.1063/1.2719967

Zhu, T.J., Zhang, S.N., Yang, S.H. & Zhao, X.B. (2010) Improved thermoelectric figure of merit of self- doped $Ag_{8--x}GeTe_6$ compounds with glass-like thermal conductivity. *Phys. Status Solidi RRL* 4, 317–319. https://doi.org/10.1002/pssr.201004278

Zukovskiy, P.W., Rodzik, A., & Shostak, Yu.A. (1997). Dielectric constant and ac conductivity of semi- insulating $Cd_{1-x}Mn_xTe$. *Semiconductors, 31*(A206), 610-614. https://doi.org/10.1134/1.1187227